ISSN 0023-1584, Kinetics and Catalysis, 2017, Vol. 58, No. 5, pp. 642–648. © Pleiades Publishing, Ltd., 2017.
Original Russian Text © M.V. Grabchenko, G.V. Mamontov, V.I. Zaikovskii, O.V. Vodyankina, 2017, published in Kinetika i Kataliz, 2017, Vol. 58, No. 5, pp. 654–661.

Effect of the Metal–Support Interaction in Ag/CeO_2 Catalysts on Their Activity in Ethanol Oxidation

M. V. Grabchenko[a], *, G. V. Mamontov[a], V. I. Zaikovskii[b], and O. V. Vodyankina[a]

[a] *National Research Tomsk State University, Tomsk, 634050 Russia*

[b] *Boreskov Institute of Catalysis, Siberian Branch, Russian Academy of Sciences, Novosibirsk, 630090 Russia*

**e-mail: marygra@mail.ru*

Received January 26, 2017

Abstract—The interaction of silver with the surface of CeO_2 in the Ag/CeO_2 catalysts prepared by coprecipitation and impregnation techniques was studied by temperature-programmed reduction, X-ray diffraction, and high-resolution transmission electron microscopy. It was shown that coprecipitation technique led to formation of strong silver–support interaction and the epitaxy of silver particles (d_{111} = 2.35 Å) on the surface of CeO_2 (d_{111} = 3.1 Å). This provided incresed catalytic activity in the oxidative dehydrogenation of ethanol at relatively low temperatures (a 15% conversion of ethanol with 100% selectivity for the formation of acetaldehyde was reached at 85°C). Above 130°C, the deep oxidation of ethanol to CO_2 becomes the predominant direction of a catalytic reaction, and the Ag/CeO_2 catalyst obtained by impregnation technique was most active in this region as a consequence of the weaker metal–support interaction.

Keywords: Ag/CeO_2 catalysts, metal–support interaction, ethanol oxidation

DOI: 10.1134/S0023158417050056

INTRODUCTION

The development of functional materials with specified properties, including catalytic activity, is currently a problem of paramount interest. The properties of a catalyst are determined in many respects by its chemical nature, the size of particles, and the distribution of active components on the support surface. The activity of supported nanostructured catalysts considerably depends on the interaction of an active component (metal) with the oxide support [1]. The possibility of controlling the strong metal–support interaction at an interface can play a decisive role in the development of catalysts with specified properties [2].

At present, considerable attention in catalysis is paid to ceria and materials on its basis. The ability of the Ce^{4+}/Ce^{3+} redox pair to activate gas-phase oxygen and the defect structure of phase boundaries (oxygen vacancy at the $Ag–CeO_2$ interface) make a direct contribution to the activity of the supported catalysts based on ceria. The Ag/CeO_2 system is a very promising catalyst for the low-temperature oxidation of organic compounds such as formaldehyde [3], CO [1, 4–6], and soot (small carbon particles) [7–12] and for the reduction of NO_x [1]. Materials based on Ag/CeO_2 are used as photocatalysts [13], and they are also used in biochemistry due to the bactericidal properties of ceria and silver [14].

However, the behavior of the Ag/CeO_2 catalysts in the reactions of selective oxidation is scantily known. Earlier, it was shown [15] that interactions between Ag nanoparticles and CeO_2 on the surface of silicon dioxide facilitate an increase in the catalyst activity in the oxidative dehydrogenation of ethanol. Thus, the variation of the strength of $Ag–CeO_2$ interaction can be an effective method for controlling the properties of silver-containing catalysts in the reactions of deep and selective oxidation of organic substances.

The aim of this work was to study the role of interfacial metal–support interaction in the Ag/CeO_2 catalysts in the reaction of ethanol oxidation. Tor control this interaction, we selected two catalyst preparation techniques: incipient wetness impregnation (when silver was introduced into the surface of an already formed phase of CeO_2) and coprecipitation, which included a redox reaction between Ag(I) and Ce(III) to strengthen the interphase interaction between the metal and the support. Temperature-programmed reduction (TPR-H_2), X-ray diffraction (XRD) analysis, (and high-resolution transmission electron microscopy (HR TEM) were used for studying the $Ag–CeO_2$ interaction and the influence of this interaction on the activity and selectivity of the Ag/CeO_2 catalysts in a reaction of ethanol oxidation.

EXPERIMENTAL

Synthesis of the Supports and Catalysts

The CeO_2 support was obtained by a precipitation technique. An aqueous solution of ammonia (NH_4OH, 25 wt %) was slowly added to 10.1 g of cerium(III) nitrate hexahydrate (analytical grade) dissolved in 150 mL of distilled water with intense stirring to reach pH 12. The resulting precipitate was filtered off, washed with distilled water, dried at 80°C for 15 h, and calcined at 500°C for 5 h.

The Ag/CeO_2 catalysts with a silver content of 10 wt % were obtained by two methods. According to the first one, silver was supported onto CeO_2 by incipient wetness impregnation (imp) with the use of an aqueous solution of silver nitrate (chemically pure). The sample obtained was designated as Ag/CeO_2 (imp). For the preparation of a catalyst with strengthened $Ag–CeO_2$ interphase interaction, a codeposition precipitation technique (coDP), which included a redox reaction between Ag(I) and Ce(III), was used [16]. For this purpose, an aqueous solution of ammonia was slowly poured into an aqueous solution of silver and cerium(III) nitrates. In this case, the precipitation of cerium(III) hydroxide occurred, and the resulting AgOH was dissolved in an excess of ammonia, being converted into the ammonium complex $Ag(NH_3)_2^+$. Then, the adsorption of this complex on the particles of cerium hydroxide occurred accompanied by the following redox reaction at pH ~12 [17]:

$$Ce(OH)_3 + Ag(NH_3)_2OH + 2H_2O = Ce(OH)_4 + Ag^0 + 2NH_4OH.$$

This was evidenced by a color change in the solution to a darker color (because of the appearance of silver nanoparticles, which absorb light in the visible region). The sample obtained was designated as Ag/CeO_2 (coDP).

The silver catalysts prepared were dried at 80°C for 15 h and calcined at 500°C for 5 h.

Characterization of the Supports and Catalysts

The low-temperature adsorption of nitrogen was used for measuring specific surface areas and pore-size distributions in the support and the catalysts. The experiments were carried out on a TriStar 3020 automatic gas-adsorption analyzer (Micromeritics, the United States).

For determining the specific surface area (S_{sp}), the multipoint (10–12 points) BET method was used in a range of the relative nitrogen pressures P/P_0 from 0.05 to 0.30. The test samples were preliminarily outgassed in a vacuum at 200°C for 120 min.

The pore size distribution was studied by the BJH method, analyzing the desorption branch of the isotherm of nitrogen adsorption–desorption.

For studying the phase composition and estimating the particle sizes (coherent scattering regions, CSR) of silver and ceria from the Scherrer equation, XRD analysis was used. The XRD analysis was carried out on a Rigaku Miniflex 600 diffractometer (Rigaku, Japan) using CuK_α radiation (λ = 1.5418 Å) and a Ni filter. The phase composition was established with the use of the PCPDFWIN database of and the POWDER CELL 2.4 software for full profile analysis.

The structure of the samples and also the morphological and crystallographic characteristics of supported silver and ceria were studied by HR TEM on a JEM–2200FS microscope (JEOL, Japan). The crystal lattice parameters were calculated by Fourier transform using the DigMicrograph (GATAN) software.

The reduction of the samples was studied by TPR-H_2 on a Chemisorb 2750 chemisorption analyzer (Micromeritics) supplied with a thermal conductivity detector using a gas mixture of H_2 + Ar (10 vol % H_2) in a temperature range from 25 to 750°C at a gas flow rate of 20 mL/min and a heating rate of 10 K/min. Before each particular experiment, the samples were subjected to oxidative pretreatment in a flow of air (20 mL/min) under temperature-programmed oxidation (TPO) conditions with heating to 500°C at a rate of 10 K/min and keeping at this temperature for 10 min.

The catalytic properties of the samples in the oxidative dehydrogenation of ethanol were studied under flow conditions at atmospheric pressure in a tubular U-shaped quartz reactor with a fixed bed of the catalyst. The granule diameter of the samples was 0.25–0.5 mm, and the sample volume was 0.5 cm^3. The reaction mixture containing 2 vol % C_2H_5OH and 18 vol % O_2 in He was passed through the catalyst bed at a rate of 60 mL/min. The concentrations of ethanol, acetaldehyde, acetic acid, diethyl ether, and ethyl acetate in the reaction mixture were measured by online gas chromatography on a Kristall 5000.2 instrument (Khromatek, Russia) supplied with a Zebron Wax plus capillary column (30 m × 0.32 mm) and a flame-ionization detector at a temperature of 160°C. A metal column packed with a Carbosieve S II polymeric porous sorbent was used for the separation of CO and CO_2, and a thermal conductivity detector was applied.

RESULTS AND DISCUSSION

The textural characteristics of the synthesized supports and catalysts were investigated by the low-temperature adsorption of nitrogen. Figure 1a shows the isotherms of nitrogen adsorption–desorption and pore size distributions for the ceria and Ag-containing catalysts. The isotherms can be related to type IV with a hysteresis in the region of relative pressures of 0.45–1.0; this fact is indicative of the mesoporous structure of the samples. The pore size was 2–10 nm in all of the samples.

The specific surface area (S_{sp}) of the ceria obtained by the precipitation tecnique was 66 m^2/g with a specific pore volume of 0.098 cm^3/g (Table 1). Upon the supporting of silver onto the surface of ceria by the impregnation method, considerable changes in the pore size distribution in the Ag/CeO_2 (imp) sample was not observed; in this case, S_{sp} decreased to 33 m^2/g and the specific pore volume, to 0.061 cm^3/g. In the Ag/CeO_2 (coDP) catalytic system, the specific surface area and the pore volume were smaller than those in CeO_2; this fact may be indicative of the interaction of silver precursors with ceria in the process of precipitation.

XRD analysis was used for determining the phase composition and estimating the sizes of silver and CeO_2 crystallites. Figure 1b shows the diffractograms of the samples based on CeO_2. The ceria and Ag/CeO_2 catalysts were characterized by the presence of reflections at $2\theta = 28.4°$, 33.8°, 47.4°, and 56.6°, which are related to the CeO_2 phase with a cubic structure. The particle size of this phase estimated from the size of CSR was 11–14 nm (Table 1). Weakly pronounced reflections at $2\theta = 38.1°$ and 44.3°, which correspond to a silver metal phase with a crystallite size of <5 nm, appeared in the spectra of the silver-containing systems. A decrease in the unit cell parameter of ceria in the Ag/CeO_2 (coDP) sample can indicate an increase in the number of oxygen vacancies in the structure of CeO_2 in the presence of silver [15] or the incorporation of Ag^+ ions (according to Belov and Bokii, the ionic radius of Ag^+ is 0.88 Å) into the lattice of CeO_2 (the ionic radius of Ce^{4+} is 1.13 Å) [18].

The reduction of the oxide states of silver and cerium in the synthesized samples was investigated by the TPR-H_2 method. The TPR profile of the CeO_2 support (Fig. 2) indicates hydrogen consumption in a range of 350–650°C, which is related to the reduction of the surface oxygen of CeO_2. The consumption of H_2 at temperatures higher than 700°C can be attributed to the reduction of the CeO_2 bulk phase to Ce_2O_3 [19, 20].

The Ag/CeO_2 catalysts mainly consume hydrogen in a range of 50–350°C. In this section, it is possible to recognize two regions of hydrogen consumption: 50–150 and 150–280°C. Peaks with maximums at 69, 120, and 132°C can be related to the reduction of silver from the oxidized clusters and highly dispersed silver oxide [21–23]. The peaks with maximums at 190 and 210°C may be attributed to the reduction of CeO_2 particles, interacting with Ag particles [15, 24]. In this case, the insignificant reduction of CeO_2 surface at temperature above 350°C was observed for the Ag/CeO_2 (coDP) and Ag/CeO_2 (imp) catalyst. A similar effect of the low-temperature reduction of ceria in

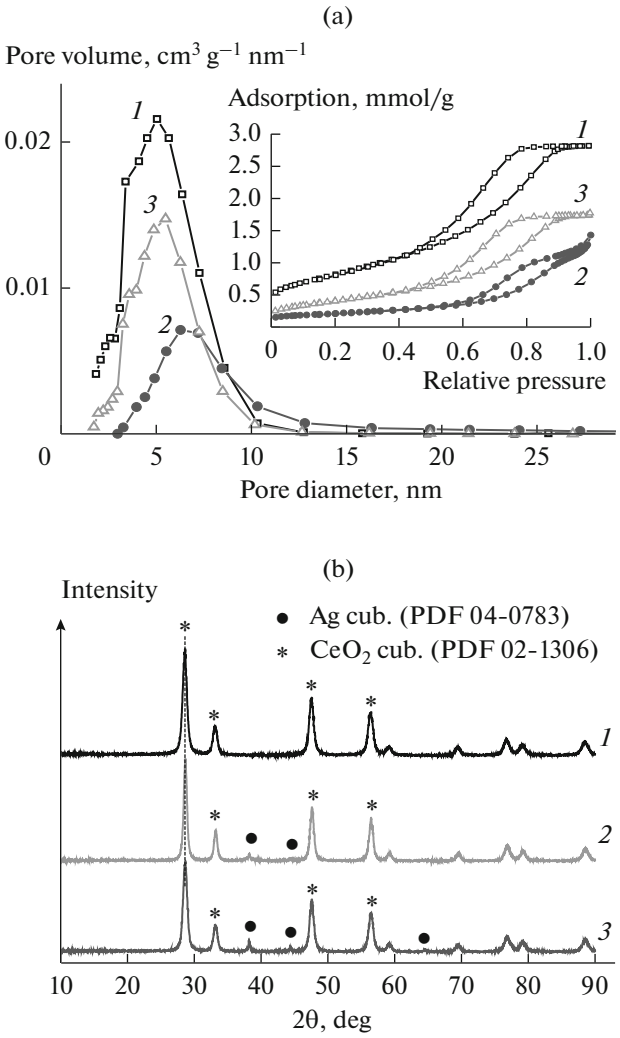

Fig. 1. (a) Isotherms of nitrogen adsorption–desorption and pore size distributions and (b) the diffractograms of the samples: (*1*) CeO_2, (*2*) Ag/CeO_2 (coDP), and (*3*) Ag/CeO_2 (imp).

Table 1. Properties of the synthesized samples

Sample	S_{sp}, m^2/g	Pore volume, cm^3/g	Pore size, nm	d_{111} (CeO_2), Å	D, nm
CeO_2 (support)	66	0.098	4.8	3.129	12.5
Ag/CeO_2 (coDP)	16	0.044	7.9	3.119	13.9
Ag/CeO_2 (imp)	33	0.061	5.2	3.124	11.4

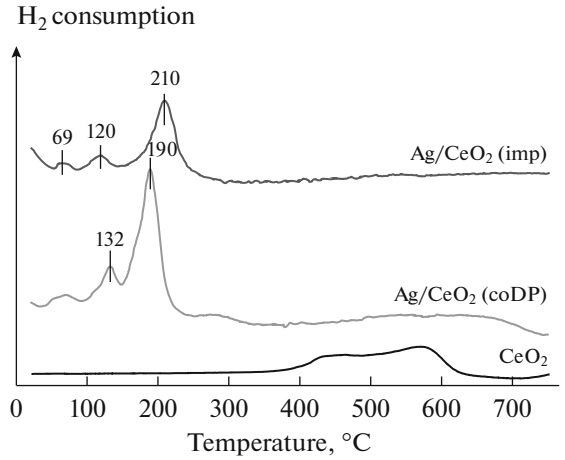

Fig. 2. TPR-H_2 profiles of the catalysts based on CeO_2 after oxidative pretreatment at 500°C.

the presence of noble metals was described previously [17, 25–27]. Thus, the results of TPR make it possible to draw the conclusion that silver partially interacts with surface of CeO_2 support. The other part of ceria surface is free from silver. In this case, the area of uncovered surface of CeO_2 particles in the catalyst obtained by the coprecipitation method is greater than that in the impregnated catalyst.

A considerable shift of the peak of surface ceria reduction in the Ag/CeO_2 (coDP) sample (a maximum at 190°C) and its higher intensity, as compared with the peak in the profile of Ag/CeO_2 (imp) (a maximum at 210°C), are indicative of the more intense interaction of silver with the surface of CeO_2 (possibly, with the introduction of Ag^+ ions into its crystal lattice). Table 2 summarizes the amounts of hydrogen absorbed under the TPR conditions. The area of a peak in the region of 50–300°C in the spectrum of the Ag/CeO_2 (imp) sample corresponds to the hydrogen absorption of 0.256 mmol/g, whereas the sample obtained by the coprecipitation method consumed somewhat more hydrogen (0.285 mmol/g) in this region. This increase is explained by the stronger interfacial interaction of silver with CeO_2, which increases the reducibility of ceria.

Table 2. Hydrogen consumption in TPR

Catalyst	T, °C	H_2 consumption, mmol/g
CeO_2 (support)	350–650	0.205
Ag/CeO_2 (coDP)	50–350	0.285
	350–650	0.124
Ag/CeO_2 (imp)	50–350	0.256
	350–650	0.026

The structure of the obtained catalysts and the distribution of an active constituent were investigated by HR TEM. Figure 3a shows the TEM image of ceria obtained by the precipitation method the CeO_2 particle size distribution in this sample. It is evident that the sample consisted of CeO_2 particle agglomerates of size 5–16 nm, which have a nearly spherical shape. The HR TEM image of the same sample (Fig. 3b) indicates that the aggregated CeO_2 particles were tightly adjoined between themselves by different faces, predominantly, by the faces (111) (d_{111} = 3.1 Å). The HR TEM study of the Ag/CeO_2 catalyst prepared by the coprecipitation method (Fig. 3c) showed that the majority of silver particles were epitaxially bound to the surface of ceria. Parallel Moiré fringes characteristic of the epitaxy of particles were observed; this corresponds to the contact of silver nanoparticles (d_{111} = 0.23 nm) of size ~2 nm with the surface of CeO_2 (d_{111} = 0.31 nm). Figure 3c shows four sections with epitaxial contacts between the metal and ceria particles. In spite of a significant difference in interplanar spacing in the lattices of silver and ceria (~25%), strong interaction between the active constituent and the support manifested itself, as judged by the observed epitaxy. In this case, the epitaxy of silver on the surface of CeO_2 is most characteristic of the crystalline metal nanoparticles of size 2–3 nm.

Figure 3e shows the HR TEM image of the Ag/CeO_2 (imp) sample. Silver occurred in this sample in the form of clusters with sizes from 0.5 to 3 nm. The model of a diffraction pattern obtained with the use of Fourier transform in the corresponding sections of images exhibited reflections in the form of ring fragments, which relate to the crystal lattice of silver (d_{111} = 0.23–0.24 nm). The ring-shaped form of the reflections can be explained by a structural disordering with a deviation from the face-centered cubic (FCC) lattice of silver, which is characteristic of a metal phase. These distortions can be a consequence of the formation of metal clusters. Only a cluster state of silver was detected in the study of a relatively large number of different sections in the granules of this catalyst.

Properties of the Catalysts in Ethanol Oxidation

The catalytic properties of the synthesized samples were investigated in the reaction of ethanol oxidation. Figure 4 shows the temperature dependence of the conversion of ethanol and selectivity for the formation of acetaldehyde and CO_x on the test samples. The formation of ethylene, acetic acid, diethyl ether, and other feasible products was not detected. The CeO_2 support exhibited its own activity (ethanol conversion, 10%) in the oxidation of alcohol starting from a temperature of ~150°C, and the complete conversion of ethanol on this sample was reached at ~235°C. In this case, the high selectivity for the formation of acetaldehyde (more than 90%) was retained to 200°C.

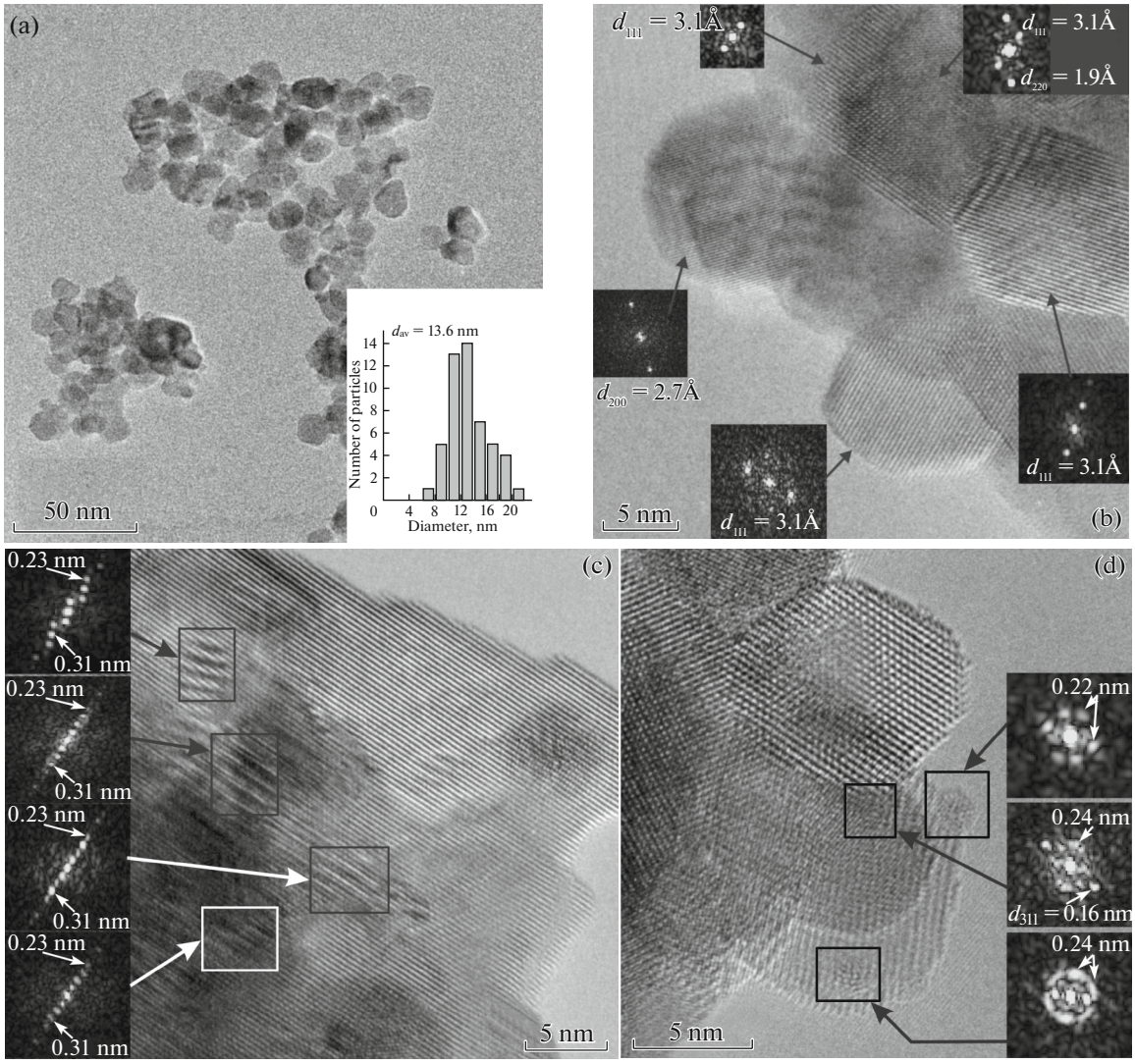

Fig. 3. TEM and HR TEM images of (a, b) the CeO_2 support and the (c) Ag/CeO_2 (coDP) and (d) Ag/CeO_2 (imp) catalysts.

A 10 and 100% conversion of ethanol over the Ag/CeO_2 (imp) sample was observed at a temperatures of 110 and 170°C, respectively. Selectivity for the formation of acetaldehyde remained at a level of 100% up to 130°C. Above 130°C, along with the oxidation of ethanol into acetaldehyde, the deep oxidation of ethanol into CO_2 is also observed.

The Ag/CeO_2 (coDP) catalyst was characterized by higher activity at a low temperature: at 85°C, the conversion of ethanol was 15% at 100% selectivity for the formation of acetaldehyde. Above 130°C, this selectivity substantially decreased because of the onset of the deep oxidation of ethanol to CO_x. The complete conversion of ethanol was achieved at ~190°C.

The higher activity of the catalyst prepared by the coprecipitation technique at relatively low temperatures can be explained by an increased rate of the recovery of active centers, as evidenced by the results of TPR in a temperature range of 90–150°C (the reduction of the oxidized states of silver). A decrease in selectivity for the formation of acetaldehyde at temperatures higher than 130°C is related to the participation of the active oxygen of ceria in the reaction at the $Ag–CeO_2$ phase boundary. This is consistent with the presence of a medium-temperature peak in the region of 100–300°C, which corresponds to the coreduction of silver and cerium oxides, in the TPR profile. The decrease in selectivity for the formation of the target product can also be caused by an increase in the binding energy of adsorbed alkoxy groups, which are reaction intermediates in the of oxidation of alcohol, on the partially reduced centers of the catalyst surface; this increases the probability of C–C bond cleavage followed by the oxidation of the resulting C_1 fragments into CO_2 [28]. Thus, the centers activated at tempera-

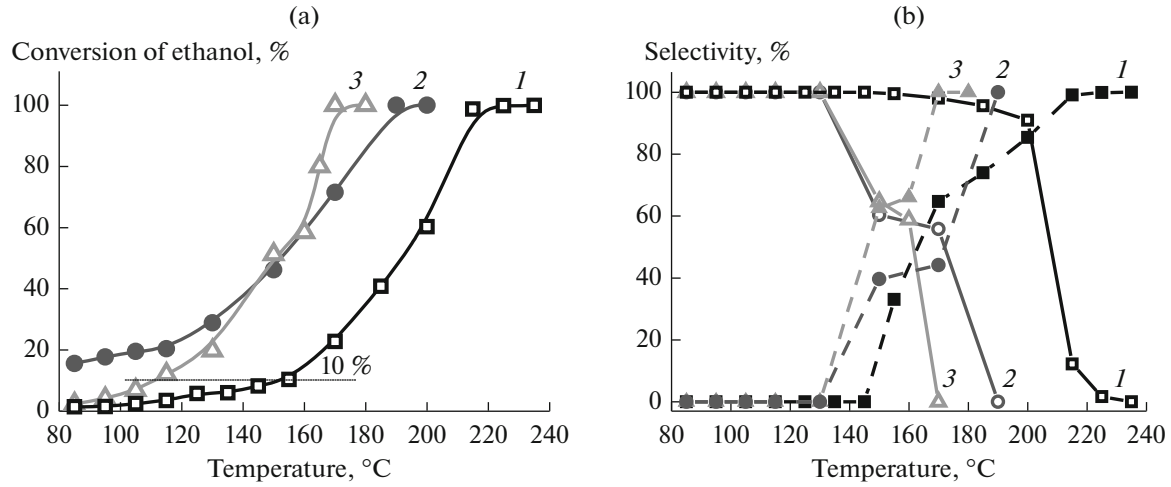

Fig. 4. The temperature dependence of (a) the conversion of ethanol in the reaction of its oxidation on the (*1*) CeO_2, (*2*) Ag/CeO_2 (imp), and (*3*) Ag/CeO_2 (coDP) samples and (b) selectivity for the formation of (solid lines) acetaldehyde and (broken lines) CO_x. Reaction mixture, ethanol : O_2 : He = 2 : 18 : 80; flow rate, 60 mL/min.

tures higher than 130°C are also predominantly the centers of deep oxidation.

Based on the experimental results, we can conclude that the interaction of silver with ceria at the Ag–CeO_2 interface influences the activity of the catalyst in the low-temperature oxidation reactions of organic substances, in particular ethanol. In a range of 85–130°C, ethanol is selectively converted into acetaldehyde; in this case, the Ag/CeO_2 (coDP) catalyst, which is characterized by the strongest metal–support interaction, is the most active. On this basis, it is possible to assume that the strong metal–support interaction, which also facilitates electron transfer between the nanoparticles of silver and ceria, is responsible for the more effective activation of alcohol molecules. A pair of the Lewis acid site $Ag^{\delta+}$ and the basic site of the oxide surface can be formed at the Ag–CeO_2 interface, and this cooperation enhances effective alcohol dehydrogenation to aldehyde with the activation of the β-C–H bond at the $Ag^{\delta+}$ sites and the O–H bond at the basic sites of ceria [16, 29, 30]. The possibility of cooperation of this kind between the silver centers and the acid–base groups of aluminum oxide was described based on the dehydrogenation of alcohols on the Ag/Al_2O_3 catalysts as an example [31].

Above 130°C, the deep oxidation of ethanol to CO_2 becomes the predominant process. This can be explained by the fact that, according to the TPR data, the surface oxygen of ceria is activated through the Ag–CeO_2 phase boundary at this temperature. Because of the high mobility of the surface oxygen of ceria, its transfer (spillover) to the Ag–CeO_2 phase boundary occurs, where the deep oxidation of alcohol supposedly takes place [1, 32]. Above 130°C, the rate of reoxidation of the surface of silver particles also increases; this fact can explain a sharp increase in the catalyst activity in the region of 130–170°C, as found earlier by Dutov et al. [33] in a study of the TPO of Ag/SiO_2. The Ag/CeO_2 (imp) catalyst is more active in this region. On the one hand, this can be explained by the fact that, according to the HR TEM data, silver in this catalyst is predominantly stabilized in the form of clusters, which more easily undergo reoxidation because of their small size. On the other hand, the weaker interaction of silver with the surface of ceria also facilitates reoxidation and, correspondingly, imparts higher activity in the reaction of deep oxidation to this catalyst, as was demonstrated using the low-temperature oxidation of CO on the Ag/SiO_2 catalyst as an example [33].

CONCLUSIONS

Thus, the control of the Ag–CeO_2 interphase interaction plays the most important role in the development of highly effective silver-containing catalysts for the selective or deep oxidation of ethanol. As demonstrated in this work, not only the particle size of the active constituent but also its interaction with the support affect the activity and selectivity of a catalyst. Stronger interaction at the Ag–CeO_2 phase boundary in the sample obtained by the coprecipitation method increases the activity of the system in the reaction of the low-temperature selective conversion of ethanol into acetaldehyde. On the contrary, the relatively weak interaction between the clusters of silver and ceria in the Ag/CeO_2 catalyst prepared by the impregnation method decreases its activity in the reaction of ethanol dehydrogenation to acetaldehyde and increases activity in the deep oxidation reaction of alcohol to CO_2.

The regularities revealed can find use in the development of catalysts for high-purity acetaldehyde pro-

duction from ethanol (because of high selectivity for acetaldehyde formation) on condition of optimizing reaction conditions to ensure a maximum yield of the target product. The catalytic systems containing silver clusters can be useful for the development of catalysts for the low-temperature deep oxidation of volatile organic substances, including CO, methanol, formaldehyde, ethanol, etc.

ACKNOWLEDGMENTS

This work was supported by a grant from the President of the Russian Federation (MK-2015.2017.3 in 2017) and Tomsk State University competitiveness improvement program (grant no. 8.2.19.2017).

REFERENCES

1. Qu, Z., Yu, F., Zhang, X., Wang, Y., and Gao, J., *Chem. Eng. J.,* 2013, vol. 229, p. 522.
2. Fu, Q. and Wagner, T., *Surf. Sci. Rep.,* 2007, vol. 62, p. 431.
3. Ma, L., Wang, D., Li, J., Bai, B., Fu, L., and Li, Y., *Appl. Catal., B,* 2014, vols. 148–149, p. 36.
4. Chang, S., Li, M., Hua, Q., Zhang, L., Ma, Y., Ye, B., and Huang, W., *J. Catal.,* 2012, vol. 293, p. 195.
5. Bera, P., Patil, K.C., and Hegde, M.S., *Phys. Chem.,* 2000, vol. 2, p. 3715.
6. Skaf, M., Aouad, S., Hany, S., Cousin, R., Abi-Aad, E., and Aboukais, A., *J. Catal.,* 2014, vol. 320, p. 137.
7. Kayama, T., Yamazaki, K., and Shinjoh, H., *J. Am. Chem. Soc.,* 2010, vol. 132, p. 13154.
8. Shimizu, K., Kawachi, H., and Satsuma, A., *Appl. Catal., B,* 2010, vol. 96, p. 169.
9. Aneggi, E., Llorca, J., Leitenburg, C., Dolcetti, G., and Trovarelli, A., *Appl. Catal., B,* 2009, vol. 91, p. 489.
10. Lee, C., Park, J., Shul, Y.-G., Einaga, H., and Teraoka, Y., *Appl. Catal., B,* 2015, vol. 174, p. 185.
11. Machida, M., Murata, Y., Kishikawa, K., Zhang, D., and Ikeue, K., *Chem. Mater.,* 2008, vol. 20, p. 4489.
12. Yamazaki, K., Kayama, T., Dong, F., and Shinjoh, H., *J. Catal.,* 2011, vol. 282, p. 289.
13. Leng, Q., Yang, D., Yang, Q., Hu, C., Kang, Y., Wang, M., and Hashim, M., *Mater. Res. Bull.,* 2015, vol. 266.
14. Wang, L., He, H., Yu, Y., Sun, L., Liu, S., Zhang, C., and He, L., *J. Inorg. Biochem.,* 2014, vol. 135, p. 45.
15. Mamontov, G.V., Grabchenko, M.V., Sobolev, V.I., Zaikovskii, V.I., and Vodyankina, O.V., *Appl. Catal., A,* 2016, vol. 528, p. 161.
16. Mitsudome, T., Mikami, Y., Matoba, M., Mizugaki, T., Jitsukawa, K., and Kaneda, K., *Angew. Chem., Int. Ed. Engl.,* 2012, vol. 51, p. 136.
17. Zhang, J., Li, L., Huang, X., and Li, G., *J. Mater. Chem.,* 2012, vol. 22, p. 10480.
18. Bokii, G.K., *Kristallokhimiya* (Crystal Chemistry), Moscow: Nauka, 1971.
19. Yao, H.C. and Yu Yao, Y.F., *J. Catal.,* 1984, vol. 86, p. 254.
20. Zhu, H., Qin, Z., Shan, W., Shen, W., and Wang, J., *J. Catal.,* 2004, vol. 225, p. 267.
21. Mamontov, G.V., Dutov, V.V., Sobolev, V.I., and Vodyankina, O.V., *Kinet. Catal.,* 2013, vol. 54, no. 4, p. 487.
22. Qu, Z., Huang, W., Cheng, M., and Bao, X., *J. Phys. Chem. B,* 2005, vol. 109, p. 15842.
23. Mamontov, G.V., Izaak, T.I., Magaev, O.V., Knyazev, A.S., and Vodyankina, O.V., *J. Phys. Chem. A,* 2011, vol. 85, no. 9, p. 1536.
24. Scire, S., Riccobene, P.M., and Crisafulli, C., *Appl. Catal., B,* 2010, vol. 101, p. 109.
25. Feio, L.S.F., Hori, C.E., Damyanova, S., Noronha, F.B., Cassinelli, W.H., Marques, C.M.P., and Bueno, J.M.C., *Appl. Catal., A,* 2007, vol. 316, p. 107.
26. Acerbi, N., Edman, TsangS.C., Jones, G., Golunski, S., and Collier, P., *Angew. Chem., Int. Ed. Engl.,* 2013, vol. 52, p. 7737.
27. Liotta, L.F., Longo, A., Macaluso, A., Martorana, A., Pantaleo, G., Venezia, A.M., and Deganello, G., *Appl. Catal., B,* 2004, vol. 48, p. 133.
28. Mullins, D.R., *Surf. Sci. Rep.,* 2015, vol. 70, p. 42.
29. Mitsudome, T., Noujima, A., Mikami, Y., Mizugaki, T., Jitsukawa, K., and Kaneda, K., *Angew Chem.,* 2010, vol. 122, p. 5677.
30. Mikami, Y., Noujima, A., Mitsudome, T., Mizugaki, T., Jitsukawa, K., and Kaneda, K., *Chem. Lett.,* 2010, vol. 39, p. 223.
31. Shimizu, K., Sugino, K., Sawabe, K., and Satsuma, A., *Chem. Eur. J.,* 2009, vol. 15, p. 2341.
32. Vayssilov, G.N., Lykhach, Y., Migani, A., Staudt, T., Petrova, G.P., Tsud, N., Skala, T., Bruix, A., Illas, F., Prince, K.C., Matolin, V., Neyman, K.M., and Libuda, J., *Nat. Mater.,* 2011, vol. 10, p. 310.
33. Dutov, V.V., Mamontov, G.V., Zaikovskii, V.I., and Vodyankina, O.V., *Catal. Today,* 2016, vol. 278, p. 150.

Translated by V. Makhlyarchuk